MOLECULAR AND CELLULAR BIOLOGY, Apr. 2004, p. 2797–2807 Vol. 24, No. 7
0270-7306/04/$08.00+0 DOI: 10.1128/MCB.24.7.2797–2807.2004
Copyright © 2004, American Society for Microbiology. All Rights Reserved.

Phosphorylation Controls Ikaros's Ability To Negatively Regulate the G_1-S Transition

Pablo Gómez-del Arco, Kazushige Maki, and Katia Georgopoulos*

Cutaneous Biology Research Center, Massachusetts General Hospital, Harvard Medical School, Charlestown, Massachusetts 02129

Received 14 November 2003/Accepted 30 December 2003

Ikaros is a key regulator of lymphocyte proliferative responses. Inactivating mutations in Ikaros cause antigen-mediated lymphocyte hyperproliferation and the rapid development of leukemia and lymphoma. Here we show that Ikaros's ability to negatively regulate the G_1-S transition can be modulated by phosphorylation of a serine/threonine-rich conserved region (p1) in exon 8. Ikaros phosphorylation in p1 is induced during the G_1-S transition. Mutations that prevent phosphorylation in p1 increase Ikaros's ability to impede cell cycle progression and its affinity for DNA. Casein kinase II, whose increased activity in lymphocytes leads to transformation, is a key player in Ikaros p1 phosphorylation. We thus propose that Ikaros's activity as a regulator of the G_1-S transition is controlled by phosphorylation in response to signaling events that down-modulate its DNA binding activity.

Ikaros encodes a family of zinc finger transcription factors which act from the earliest stages of hemo-lymphopoiesis and are required for the balanced production and function of a variety of blood and immune cells (6, 9). Hemopoietic stem cell activity is reduced in Ikaros-null mice, and further differentiation along the lymphoid pathways is impaired. Significantly, Ikaros-null mice lack all B lymphocytes and fetal T-lineage cells, and only a small number of T-cell precursors are detected in the thymus after birth (1, 6). In sharp contrast, the numbers of myeloid precursors and of their terminally differentiated progeny are increased in the absence of Ikaros (25). Taken together, these studies suggest that Ikaros plays a critical role at pivotal points of the hemopoietic pathway and is responsible for lymphoid versus myeloid differentiation (9).

Ikaros activity is also required at subsequent stages of differentiation along the T-cell pathway. The small number of postnatal T-cell precursors detected in the thymus of Ikaros-null mice can progress to the double-positive (DP) stage and to an apparent $CD4^+$ single-positive (SP) stage of differentiation in the absence of pre-T-cell receptor (TCR) signaling (35). In the presence of TCR signaling, an increase in the number of $CD4^+$ SP thymocytes is detected, accompanied by a decrease in DP thymocytes (34). The presence of this aberrant $CD4^+$ SP thymocyte population in Ikaros-null mice reflects the inability of a significant fraction of DP cells to express CD8, implicating Ikaros in the activation of this lineage-specific marker (13).

There also appears to be a direct correlation between levels of Ikaros activity and production of lymphocyte precursors. In mice heterozygous for the Ikaros-null mutation, a 50% reduction in Ikaros protein causes a 50% reduction in lymphocyte precursors. Homeostatic mechanisms that operate at later stages of the lymphoid pathway provide for mature lymphocyte populations that appear normal in number and cell surface phenotype. Nonetheless, these apparently normal mature T cells enter the cell cycle under minimal TCR engagement events and proliferate robustly compared to their wild-type counterparts (2). Consistent with this hyperproliferative phenotype, mice haploinsufficient for Ikaros develop T-cell leukemias and lymphomas (35, 36).

Ikaros exerts its effects in development as a set of differentially spliced isoforms that contain two functionally distinct Kruppel-type zinc finger domains, one involved in DNA binding and the second involved in protein interactions (24, 31). Of the Ikaros isoforms described thus far, Ik-1 and Ik-2 are the most abundantly expressed throughout development and contain distinct combinations of DNA-binding zinc finger modules. Thus, in normal hemopoietic cells and mature lymphocytes, most of the Ikaros isoforms can bind DNA. In lymphocytes, the majority of Ikaros protein is present in higher-order complexes that contain chromatin remodellers and chromatin-modifying enzymes (16, 18, 20). A major fraction of the lymphoid Ikaros protein is associated with components of the NURD complex that include the ATP-dependent chromatin remodeller Mi-2β and histone deacetylase 1 (HDAC-1) and HDAC-2. A significant fraction of Ikaros protein is also associated with the SWI/SNF remodeling complex in lymphocytes (16).

Given the importance of Ikaros activity in lymphocyte development and proliferation, we investigated whether Ikaros proteins are posttranslationally modified and whether such modifications affect their function. Here we provide new evidence that Ikaros functions as a negative regulator of the G_1-S transition and that this activity is controlled in a cell cycle-dependent manner through phosphorylation of a serine/threonine-rich region in exon 8. Casein kinase II (CKII) is predominantly responsible for these Ikaros phosphorylation events that impact its cell cycle regulatory function, possibly by reducing its affinity for DNA.

* Corresponding author. Mailing address: Cutaneous Biology Research Center, Massachusetts General Hospital, Harvard Medical School, Charlestown, MA 02129. Phone: (617) 724-8279. Fax: (617) 726-4453. E-mail: katia.georgopoulos@cbrc2.mgh.harvard.edu.

MATERIALS AND METHODS

Reagents, plasmids, and cell lines. The cell cycle inhibitors mimosine, thymidine, hydroxyurea, and nocodazole were purchased from Sigma-Aldrich. The

protein kinase inhibitors apigenin, emodin, 5,6-dichlorobenzimidazole riboside (DRB), H-89, KN-62, bisindolylmaleimide I (BSMI), olomoucine, and roscovitine were purchased from Alexis Biochemicals. Drug treatments are indicated in every experiment. Recombinants λ phosphatase (PPase) and CKII were obtained from New England Biolabs. The CMV2-FlagIk-1 plasmid has been previously described (18). Ik-1 and Ik-2 cDNAs were cloned at XhoI and NotI positions of the poly-linker in the retrovirus pMX-GFP-IRES, kindly provided by T. Kitamura, Tokyo University (26). All of the mutations described in this paper were generated by using the Stratagene directed mutagenesis kit according to the manufacturer's recommendations. Lymphoid cell lines and primary T cells were maintained in RPMI medium, supplemented with 10% fetal bovine serum (FBS; HyClone). The Phoenix, 293T, and NIH 3T3 cell lines were maintained in Dulbecco's modified Eagle's medium with 10% FBS.

Transfections and infections. 293T cells were transfected by the HBS-$CaPO_4$ method as previously described (20). Cells were harvested 36 to 48 h after transfection. For infections, retroviruses were generated after transfecting the packaging cell line Phoenix with pMX-GFP-IRES plasmid or the Ikaros-expressing derivatives. Forty-eight hours after transfection, viral supernatants were recovered and used to infect NIH 3T3 cells. Infected cells were harvested 48 to 72 h after infection.

In vivo and in vitro phosphorylation studies of Ikaros and phosphopeptide mapping. For the in vivo Ikaros phosphorylation studies, lymphoid cells or Ikaros-transfected 293T cells were incubated with radioactive orthophosphate for the indicated times. For the in vitro Ikaros phosphorylation studies, purified Ikaros proteins were incubated with 5 U of recombinant CKII for 30 min at 30°C in the presence of [γ^{32}P]ATP, following the manufacturer's recommendations. Ikaros phosphopeptide and phosphoamino acid mapping were carried out as previously described (3). After immunoprecipitation, Ikaros proteins were resolved by sodium dodecyl sulfate-polyacrylamide gel electrophoresis (SDS-PAGE) and transferred to nitrocellulose membranes, which were subjected to autoradiography to reveal the radioactive signal. Ikaros protein levels were detected by Western blotting. The Ikaros band was excised from the membrane and subjected to proteolytic digestion with trypsin. The resulting peptides were then separated in two dimensions in a thin-layer chromatography plate. The first dimension involved electrophoresis (pH 8.9 buffer), and the second dimension involved chromatography in isobutyric acid buffer (3). Thin-layer chromatography plates were then subjected to autoradiography.

Western blot and gel shift. Nuclear or whole-cell extracts were prepared as previously described (16, 20). The proteins were separated by SDS-PAGE and transferred to membranes. The membranes were probed with the relevant antibodies and examined by enhanced chemiluminescence with the ECL system. The antibodies used were Flag M2 (Sigma), YY1 (Santa Cruz), and anti-Ikaros (16). DNA mobility shift assays were performed as previously described (31). The C69 oligonucleotide containing a high-affinity Ikaros binding site was used (31). The labeled oligonucleotide was incubated with FlagIk-1 protein or the indicated mutants expressed in 293T cells and isolated by Flag column purification. For supershift assay, the anti-Ikaros antibody was used.

Cell cycle analysis. Drugs for cell cycle arrest were used as previously described (21). Cell cycle profiles were analyzed by DNA staining. Cells were fixed in 95% ethanol, resuspended in staining solution containing 50-μg/ml propidium iodide (PI) and 100-μg/ml RNase A, and incubated at 37°C for 30 min. DNA content (PI) was analyzed by flow cytometry on a FACScan (Becton Dickinson). Where indicated, mimosine, hydroxyurea, or nocodazole was added before harvesting.

RESULTS

Ikaros proteins are hyperphosphorylated: mapping of Ikaros phosphorylation sites. Given that the level of Ikaros activity is a critical determinant of differentiation and proliferation in the hemo-lymphoid system, we examined whether the protein underwent posttranslational modifications such as phosphorylation. A T-cell line that expresses a Flag-tagged Ikaros isoform (FlagIk-7) that associates through its C-terminal zinc fingers with endogenously produced Ikaros proteins (16) was grown in the presence of radioactive orthophosphate. Using antibodies to the Flag epitope, Ik-7 and its associates were immunoprecipitated from asynchronously growing cells and resolved by SDS-PAGE. The full-length Ik-1 isoform obtained through this strategy was trypsinized and subjected to two-dimensional phosphopeptide mapping (3). Three groups of phosphopetides were detected (Fig. 1A, p1, p2, and p3). p1 and p2 were single phosphopeptides, whereas p3 comprised several phosphopeptides, which were present on average at lower abundance. A similar phosphorylation pattern for Ik-1 was seen in the B- and T-cell lines Bal17 and Rml11 (data not shown). The Ikaros p1 to p3 phosphopeptides were also detected when the Ik-1 protein was ectopically expressed in the epithelial line 293T (Fig. 1B), indicating that these phosphorylation events were not lymphoid specific.

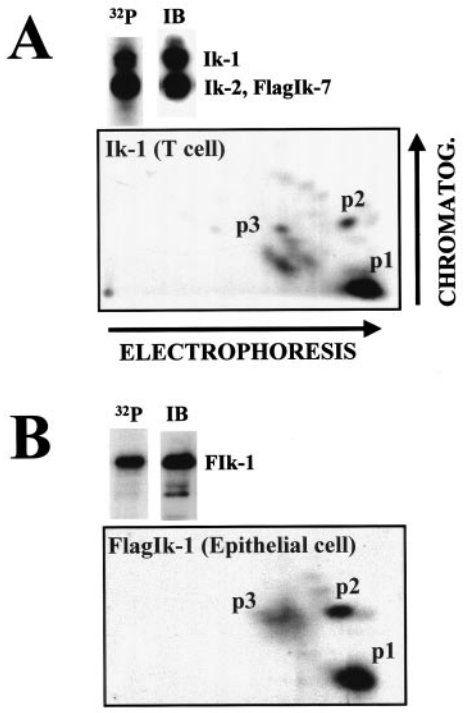

FIG. 1. The Ikaros phosphorylation pattern in lymphoid and nonlymphoid cells. (A) The T-cell line 510 was labeled in vivo with radioactive orthophosphate for 12 to 16 h. After immunoprecipitation (IP), Ikaros proteins were resolved by SDS-PAGE and transferred to nitrocellulose membranes. Radioactive signal was revealed by autoradiography of the membranes (^{32}P), and proteins were determined by immunoblotting (IB) of the same membranes with anti-Ikaros antibody. The Ik-1 isoform was trypsinized, and the resulting peptides were separated first by electrophoresis and then by chromatography (CHROMATOG.) (3). The phosphorylated peptides were revealed by autoradiography. (B) 293T cells (epithelial cell line) were transfected with 5 μg of CMV2-FlagIk-1. Thirty-six hours posttransfection, cells were labeled with radioactive orthophosphate for an additional 12 to 16 h. After immunoprecipitation, FlagIk-1 was processed like in panel A. The major regions of phosphorylation 1, 2, and 3 (p1, p2, and p3, respectively) are indicated.

The theoretical mobilities of Ikaros p1 and p2 were calculated by standard procedures (3), and the region from which they were derived was deduced (Fig. 2A, p1 and p2). The location of Ikaros p1 was estimated to be within Ikaros exon 8 between amino acids 383 and 404 ($_{383}$EASPSNSCQDSTDT ESNAEEQR$_{404}$) upstream of the C-terminal zinc fingers. The location of Ikaros p2 was mapped in exon 4 between amino acids 59 and 69 ($_{59}$VETQSDEENGR$_{69}$) in a putative phosphorylation site at position S63 (Fig. 2A). Deletion of the 383-

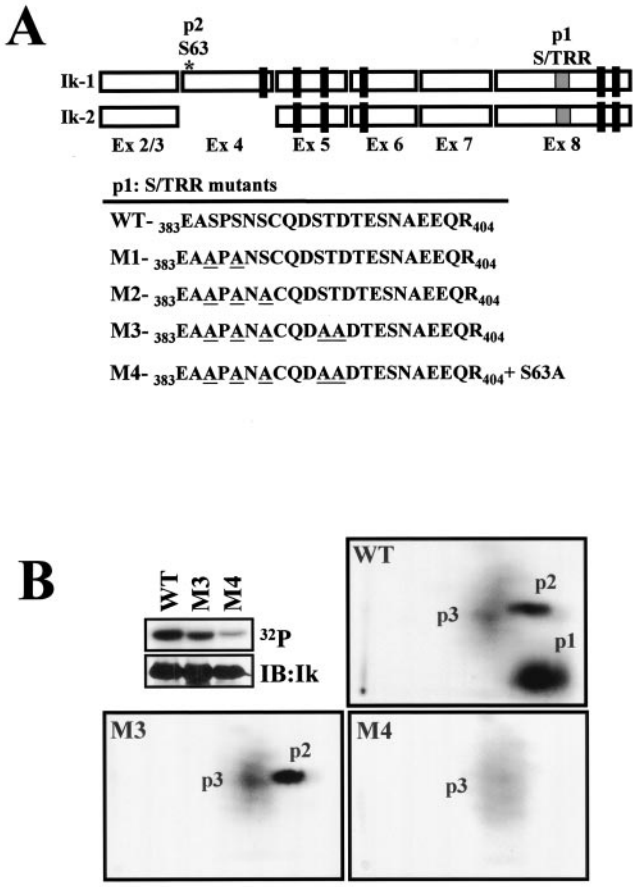

FIG. 2. Characterization of the major phosphorylated residues in Ikaros. (A) Representation of Ik-1 and Ik-2 isoforms indicating the theoretical positions of phosphopeptides 1 and 2 (p1 and p2, respectively). Mutations M1 to M3 generated in the S/T-rich region (S/TRR) of p1 are also shown. Mutant M4 was generated by combining mutations M3 and S63 to A (S63A). (B) 293T cells were transfected with either CMV2-FlagIk-1 (wild type [WT]) or the mutants FlagIk-1-M3 (S385, S387, S389, S393 and T394 to A) and FlagIk-1-M4 (S63, S385, S387, S389, S393, and T394 to A) and grown in the presence of radioactive orthophosphate for 16 h. Cells were then harvested, and Ikaros proteins were immunoprecipitated, separated by SDS-PAGE, and transferred to nitrocellulose. Their phosphorylation level was revealed by autoradiography (^{32}P), and the protein level was detected by Western blotting with anti-Flag antibodies (IB:Ik). The phosphopeptide mappings of the following proteins are shown: wild type (WT), S/T of p1 to A (M3) and S63 of p2, and S/T of p1 to A (M4). Three major phosphopeptides (p1, p2, and p3) were detected.

to 404-amino-acid region abrogated p1, in agreement with the theoretical calculations (data not shown). Using a phosphoamino acid technique (3), we determined that this peptide was phosphorylated in one threonine and three to four serines (data not shown). Since this part of the Ikaros protein is a serine (S)- and threonine (T)-rich region (S/TRR; five S residues and two T residues) with several putative phosphorylation sites, a series of mutations were generated in p1 (M1, S385 and S387 to A; M2, S385, S387, and S389 to A; and M3, S385, S387, S389, S393, and T394 to A). The Ikaros M1 to M3 proteins were ectopically expressed in 293T cells, which exhibit an Ikaros phosphorylation pattern similar to that in lymphoid cells (Fig. 1), and the level of phosphorylation and the peptide pattern were examined. As shown in Fig. 2B, the phosphorylation level of the Ik-1-M3 protein that contains mutations in all five putative phosphorylation sites was significantly reduced relative to the wild type. Furthermore, the M3 mutant displayed a complete loss of p1 (Fig. 2B, M3). In contrast, the Ik-1M1 and -M2 mutants with mutations in a subset of the putative phosphorylation sites in this region exhibited a progressive reduction in p1 signal level as well as a change in p1 mobility (data not shown). A mutation of S63 to A (S63A) was also introduced in combination with the M3 serine and threonine mutations (Fig. 2A, M4). This mutation further reduced the Ik-1 phosphorylation levels and ablated the p2 signal (Fig. 2B, M4).

Thus, in asynchronously dividing cells, there are two major Ikaros phosphorylation regions. These Ikaros phosphorylation events, which involve S63 in the alternatively spliced exon 4 and a combination of five S/T residues within amino acids 385 to 394 in the shared exon 8, do not appear to be restricted to lymphocytes.

CKII is mainly responsible for Ikaros phosphorylation at p1 and p2. The Ikaros p1 and p2 phosphopeptides contain consensus sites for several known serine/threonine kinases (Fig. 3A). There are two putative CKII sites in p1 (S389 and T394) and one site in p2 (S63). In addition, p1 contains one consensus site for a cyclin-dependent kinase (cdk), protein kinase A (PKA), or Ca^{2+} calmodulin-dependent kinase II (CaMKII) at S385 and three sites for glycogen synthase kinase 3 (GSK3) at S385, S389, and T394.

We next investigated whether any of these kinases are responsible for Ikaros p1 and p2 phosphorylation (Fig. 3B and C). 293T cells expressing Ikaros were pretreated for 1 h with kinase-specific inhibitors and then labeled with radioactive orthophosphate for an additional 2 h. Inhibitors of cdks and GSK3 reduced Ikaros phosphorylation by 2- and 1.5-fold, respectively (Fig. 3B, cdk-Rosc.+olo and GSK3-LiCl). Inhibitors of CKII gave a dramatic 4.3-fold reduction in Ikaros phosphorylation (Fig. 3B, CKII-Ap.+DRB). Reduction of Ikaros phosphorylation by the CKII inhibitors was manifested in the p1 and p2 regions, both of which have CKII sites (Fig. 3B, p1 and p2/Ap.+DRB). p3 phosphorylation was also reduced with this treatment, indicating that p3 phosphopeptides were also dependent upon CKII activity. The combination of CKII, cdk, and GSK3 inhibitors did not provide any further reduction in Ikaros phosphorylation (Fig. 3B, All). In contrast to the CKII inhibitors, inhibitors of PKA, CaMKII, and protein kinase C (PKC) had no effect on Ikaros phosphorylation (Fig. 3C, H-89, KN-62, and BSMI). Taken together, these data suggest that CKII is predominantly responsible for Ikaros phosphorylation in p1, p2, and p3. GSK3 and cdk also contribute to the p1 phosphorylation events.

To determine whether Ikaros is a direct substrate of CKII, purified wild-type Ikaros and the p1 (M3), p2 (S63A), and p1+p2 (M4) phosphorylation mutants were used as substrates for recombinant CKII in vitro (Fig. 3D). The level of phosphorylation in the Ikaros mutants was reduced relative to the wild-type protein (Fig. 3D, compare lanes S63A, M3, and M4 versus wild type). Furthermore, phosphopeptide mapping of the Ikaros mutants show that p1 and p2 were also sites for CKII activity in vitro. In the absence of the p1 and p2 phosphorylation sites (Fig. 3D, M3, S63A, and M4), Ikaros phos-

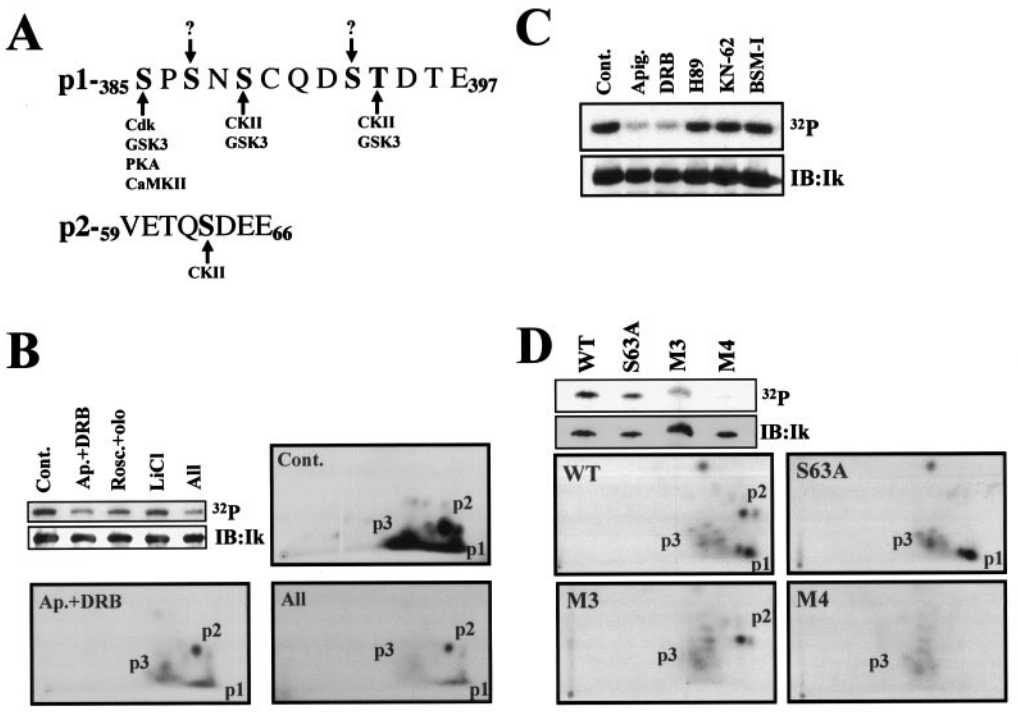

FIG. 3. Ikaros is a substrate of CKII: in vivo and in vitro studies. (A) Graphical representation of kinase consensus sites in p1 and p2. (B) FlagIk1-expressing 293T cells were treated with 20 μM apigenin, 5 μM emodin, and 50 μM DRB (Ap.+DRB) to inhibit CKII (4, 37); 50 μM roscovitine and 50 μM olomoucine (Rosc.+olo) to inhibit cdks; 10 mM LiCl to inhibit GSK3; or all of the drugs together (All). Phosphopeptide mappings of trypsinized Ikaros from the "Cont.," "Ap.+DRB," and "All" samples were performed as described in the legends to Fig. 1 and 2. (C) 239T cells expressing FlagIk-1 were treated with vehicle (dimethyl sulfoxide control [Cont.]), 40 μM apigenin plus 10 μM emodin (Apig.), 50 μM DRB, 10 μM H-89 to inhibit PKA, 10 μM KN-62 to inhibit CaMKII, or 10 μM BSMI to inhibit PKC. Proteins were separated by SDS-PAGE, transferred to nitrocellulose membranes, and exposed to reveal phosphate incorporation (^{32}P). Ikaros protein levels were determined by immunoblotting with anti-Flag antibodies (IB:Ik). (D) Purified FlagIk1 (wild type) and the mutant variants FlagIk-1-S63A (S63A), FlagIk-1-M3, or FlagIk-1-M4 proteins were incubated in vitro with recombinant CKII. Phosphopeptide mappings of trypsinized Ikaros proteins were performed like in panel B. The major phosphopeptides (p1, p2, and p3) are shown in panels B and D.

phorylation levels by CKII in vitro were dramatically reduced. The residual Ikaros phosphorylation in the absence of p1 and p2 was contributed by the p3 phosphopeptides (Fig. 3D, M4).

Taken together, these data show that Ikaros phosphorylation at p1 and p2 regions in vivo is predominantly due to the direct action of CKII. GSK3 and cdk may also contribute to the Ikaros p1 phosphorylation events.

Ikaros phosphorylation undergoes a dynamic change during the G_1-S transition. We next examined whether cell cycle transitions induce changes in Ikaros phosphorylation. Since the patterns of Ikaros phosphopeptides are similar between asynchronously dividing lymphoid and nonlymphoid cells, we first examined potential changes in Ikaros phosphorylation during the cell cycle in 293T cells. Ikaros-expressing 293T cells were treated with mimosine, hydroxyurea, and nocodazole, which, respectively, arrest cells in the late G_1, S, and M phases, or were left untreated (Fig. 4A, top panels). Flow cytometric analysis confirmed that the majority of cells treated with mimosine were in late G_1 (65%), cells treated with hydroxyurea were in S (57%), and cells treated with nocodazole were in M (79%) (Fig. 4A). In the asynchronously growing population, 46% of cells were in G_1, 22% in S, and 32% in G_2/M (Fig. 4A).

Strikingly, Ikaros protein was found in a dephosphorylated state in late-G_1-arrested cells (Fig. 4A, middle panel, Mimos.). Phosphopeptide mapping of Ikaros in these cells revealed a severe reduction in the signal of all phosphopeptides, both major and minor ones, which are readily detected in the asynchronously growing population (Fig. 4A, bottom). This reduction in Ikaros phosphorylation was also observed in cells treated with an excess of thymidine, which also arrests cells in the late G_1 phase (data not shown). In sharp contrast, phosphopeptide mapping of Ikaros from S-phase cells (hydroxyurea treated) indicated that the protein undergoes de novo phosphorylation at p1, p2, and p3, as cells transit from the G_1 into the S phase of the cell cycle. Ikaros is also phosphorylated at p1 to p3 at the M phase of the cell cycle (Fig. 4A, Nocod.). Upon longer exposure of the phosphopeptide maps, additional phosphopeptides are detected (data not shown), which likely represent the recently reported M-phase phosphorylation events at the linker region of the Ikaros N-terminal DNA binding zinc fingers (7).

We next examined whether similar changes in Ikaros phosphorylation were taking place in cycling lymphocytes. The phosphorylation status of endogenous Ikaros proteins was examined in the T-cell line 510 (Fig. 4B). As with Ikaros protein ectopically expressed in the 293T epithelial cells, phosphorylation of isoforms isolated from late G_1-arrested (mimosine treated) T cells was drastically reduced, whereas those iso-

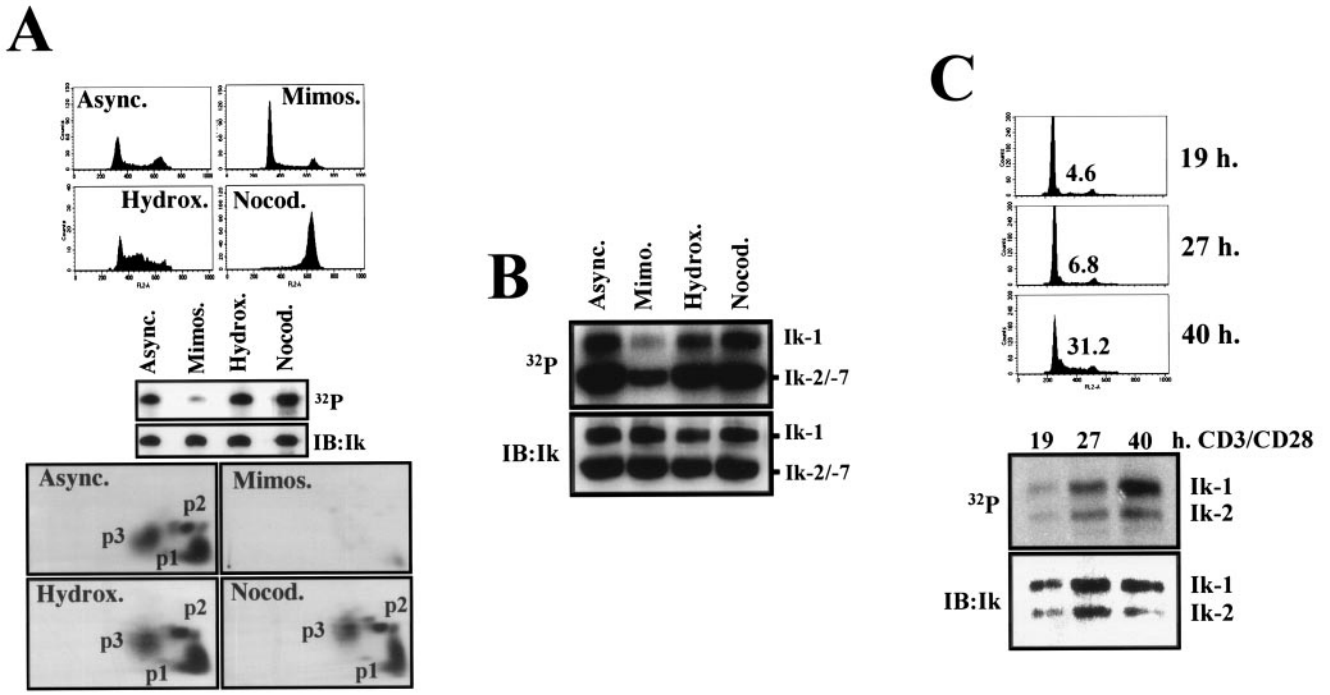

FIG. 4. Ikaros phosphorylation is dynamically regulated during the cell cycle. (A) 293T cells were transfected with CMV2-FlagIk-1. Thirty-six hours after transfection, cells were incubated for an additional 20 h with or without 0.2 mM mimosine (Mimos., late G_1-phase arrest), 1 mM hydroxyurea (Hydrox., S-phase arrest), or 0.5-μg/ml nocodazole (Nocod., M-phase arrest). A fraction of cells were stained with PI and analyzed for their cell cycle profiles by flow cytometry (upper). The rest of the cells were treated in the presence of radioactive orthophosphate and subjected to immunoprecipitation for Ikaros proteins. Proteins were separated by SDS-PAGE and then transferred to nitrocellulose membranes, which were exposed to reveal phosphate incorporation (^{32}P, middle). Ikaros protein levels were determined by immunoblotting with anti-Ikaros antibodies (IB:Ik, middle). Phosphopeptide mappings are shown (lower). (B) Cells of the 510 line were treated for 14 h with or without the indicated drugs in the presence of radioactive orthophosphate. Immunoblot analysis and radioactive signal detection were performed as in the middle section of panel A. (C) Primary T lymphocytes were isolated from spleen and mesenteric lymph nodes from 4- to 6-week-old mice. T cells were activated with plate-bound anti-CD3 plus CD28 antibody for the indicated times, and radioactive orthophosphate was added 2 h before harvesting. Analysis of Ikaros proteins was performed as in panel B. Cell cycle profiles and the percentage of cells in S phase are shown (upper). The positions of the Ikaros isoforms 1, 2, and 7 (Ik-1, -2, and -7, respectively) are indicated. Async., asynchronously growing population.

forms isolated from T cells arrested in the S and M phases (hydroxyurea or nocodazole treated) of the cell cycle and from an asynchronously growing culture were hyperphosphorylated (Fig. 4B). Phosphopeptide mapping analysis of Ik-1 in these stage-arrested T cells gave a similar pattern of phosphorylation compared to Ik-1 ectopically expressed in 293T cells (data not shown).

The regulation of Ikaros phosphorylation was also studied in activated primary lymphocytes. T lymphocytes isolated from spleen and lymph nodes of adult mice were treated with anti-CD3 plus anti-CD28 antibodies, and endogenous Ikaros phosphorylation was evaluated at different time points after receptor engagement. At 19 to 27 h of activation, the majority of T cells were in mid-to-late G_1 (93 to 95%), and a low level of Ikaros phosphorylation was detected. At 40 h of stimulation, more than 30% of the T cells had entered S phase, and a dramatic increase in Ikaros phosphorylation was noted (Fig. 4C).

Taken together, these data demonstrate that the phosphorylation status of Ikaros is dynamically regulated during the cell cycle in both lymphoid and nonlymphoid cells. Ikaros is present in a dephosphorylated state during late G_1 phase, becomes hyperphosphorylated as cells enter the S phase, and remains so through the M phase of the cell cycle.

Ikaros phosphorylation regulates its ability to control the G_1-S transition. Ikaros DNA binding activity inversely correlates with the ability of primary lymphocytes to undergo proliferative responses (2, 35). Genetic mutations that reduce the level of Ikaros DNA binding isoforms in quiescent T cells facilitate their activation (G_1 entry) at reduced levels of antigen receptor-mediated signaling and accelerate the transition from G_1 into S phase (2, 35). Cell cycle-dependent changes in Ikaros phosphorylation may be a physiological way by which lymphocytes control their ability to cycle. According to this hypothesis, Ikaros may exist in two states: a dephosphorylated active form that impedes cell cycle entry and a phosphorylated inactive form that is more permissive to cell cycle progression. We examined this hypothesis by studying the effect that wild-type Ikaros isoforms and their phosphorylation mutants have on the cell cycle.

The DNA binding isoforms Ik-1 and Ik-2 were ectopically expressed with the pMX-GFP (green fluorescent protein) retroviral vector in mouse NIH 3T3 fibroblasts, which are amenable to studies of growth regulation (27). Prior to these stud-

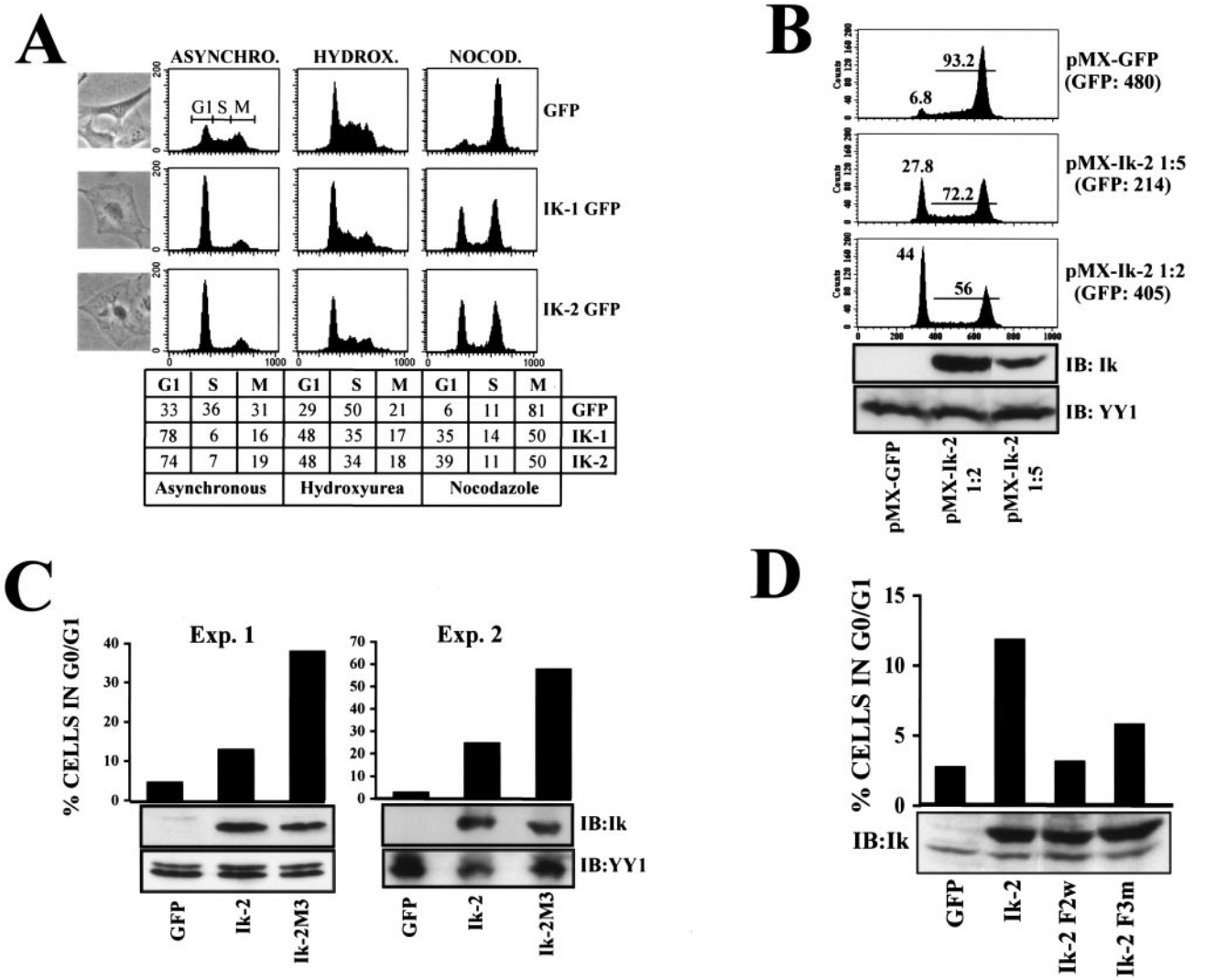

G1	S	M	G1	S	M	G1	S	M	
33	36	31	29	50	21	6	11	81	GFP
78	6	16	48	35	17	35	14	50	IK-1
74	7	19	48	34	18	39	11	50	IK-2
Asynchronous			Hydroxyurea			Nocodazole			

FIG. 5. Ikaros arrests cells in the G_1 phase of the cell cycle, and phosphorylation alleviates this effect. (A) Flow cytometric cell cycle profiles of NIH 3T3 cells infected with pMX-GFP-IRES (GFP), pMX-Ik-1-GFP-IRES (Ik-1 GFP), or pMX-Ik-2-GFP-IRES (Ik-2 GFP). Cells were left untreated (asynchronous [ASYNCHRO.], right column) or treated with 1 mM hydroxyurea (HYDROX., middle column) or 0.5-μg/ml nocodazole (NOCOD., left column) to arrest cells in the S or M phase, respectively. The percentage of cells in the G_0-G_1 (G_1), S, or G_2/M (M) phases under the different conditions is depicted in the table at the bottom of the panel. Photomicrographs of representative asynchronously growing cells, infected under each condition, are shown. (B) NIH 3T3 cells were infected with Ik-2 retroviruses at 1:5 or 1:2 dilutions in fresh medium. Seventy-two hours after infection, GFP-positive cells were sorted and treated with nocodazole for an additional 16 h. The percentages of cells remaining in the G_1 or S + M phases are represented. The level of expressed Ik-2 protein was determined by immunoblotting with anti-Ikaros antibody (IB:Ik). The YY1 protein level is shown as a loading control. The GFP mean fluorescence is shown in parentheses. (C) NIH 3T3 cells were infected with the indicated retroviruses, and 72 h after infection, cells were treated as in panel B. Results from two representative experiments out of six performed with similar results are shown. (D) NIH 3T3 cells were infected with the indicated retroviruses. Seventy-two hours after infection, cells were treated as in panel B. Results from one representative experiment out of three performed with similar results are displayed.

ies, we established that in NIH 3T3 fibroblasts, Ikaros underwent similar phosphorylation events involving the p1 and p2 peptides, albeit at a much-reduced level compared to the epithelial 293T cells (data not shown). After 72 h of infection of NIH 3T3 fibroblasts with control or Ikaros recombinant viruses, 90 to 92% of the cells were GFP positive. Of the cells infected with an empty retrovirus, 36% were in S phase and 31% were in G_2/M, whereas 33% were in G_1, a profile that is representative of an actively growing population (Fig. 5A, GFP). In sharp contrast, the great majority of cells infected with either Ik-1 or Ik-2 were in the G_1 phase (Fig. 5A, Ik-1, 78%; and Ik-2, 74%). To further demonstrate that Ikaros-infected fibroblasts were blocked in G_1, cells were treated for 20 h with hydroxyurea and nocodazole, which block at the S and M phases, respectively (Fig. 5A). Of the cells infected with the empty retrovirus and treated with hydroxyurea, 29% were in G_1 and 50% were in S phase, whereas similarly treated cells expressing Ik-1 and Ik-2, were 48% in G_1 and 35% were in S phase. Of control cells treated with nocodazole, 6% were in G_1 and 81% were in the G_2/M phase (Fig. 5A), whereas 35 to 39%

of cells expressing Ik-1 or Ik-2 were in G_1. It has been previously reported that NIH 3T3 fibroblasts arrested in the late G_1 phase of the cell cycle exhibit a characteristic flat-cell morphology (38, 39). This morphology reflects the expanded cytoplasm of a cell ready to replicate its DNA (14). Cells expressing Ikaros proteins also presented a flat morphology, demonstrating that Ikaros arrests cells in the late G_1 phase of the cell cycle (Fig. 5A).

We next examined whether the extent of cell cycle arrest was dependent on Ikaros protein levels. NIH 3T3 fibroblasts were infected with two different titers of the Ik-2-expressing retrovirus (Fig. 5B, 1:2 and 1:5 dilutions of pMX-Ik-2 stock). The 1:2 dilution of the retrovirus infected 82% of the cells, whereas the 1:5 dilution of retrovirus infected only 30% of the cells. Western analysis of the GFP-expressing cells obtained in these studies confirmed that Ikaros (and GFP) protein expression was correlated with the retroviral titer (Fig. 5B, Ik panel). These observations are in agreement with previously described results (17). The GFP-positive cells were sorted and further analyzed for cell cycle profiles after treatment with the M-phase blocker nocodazole. Significantly, the number of cells in the G_1 phase appeared to be dependent on Ikaros protein levels (Fig. 5B, Ik-2, 1:5; and Ik-2, 1:2). In the absence of any Ikaros expression, only 7% of the GFP-positive cells (infected with pMX-GFP) were in G_1. The number of cells in G_1 increased to 28% when cells were infected with the lower titer of the Ikaros-expressing retrovirus (pMX-Ik-2, 1:5) and to 44% when infected with the higher titer (pMX-Ik-2, 1:2). Thus, the extent of the G_1 arrest caused by Ikaros was dependent on its protein level.

While both of the Ikaros DNA binding isoforms, Ik-1 and Ik-2, provide a G_1 arrest, only Ik-1 contains both of the phosphorylation sites described above. We therefore examined whether phosphorylation mutants at the shared region in exon 8 influences Ikaros's ability to regulate the G_1-S transition in the context of Ik-2. To assess potential enhancing effects of the Ikaros mutations on the ability of the protein to block the cell cycle, infection conditions were used in which lower levels of Ik-2 or its M3 mutant variant were expressed in a fraction of NIH 3T3 cells. In two separate experiments (shown in Fig. 5C), vector control-infected cells treated with nocodazole displayed a 3 to 5% distribution in G_1, which increased to 12 to 25% in the Ik-2-expressing populations, indicating an Ikaros-dependent partial block in G_1 consistent with previous findings. Significantly, in the same study, the G_1 distribution of the Ik-2-M3 mutant-expressing cells was increased to 32 to 56%, respectively, indicating a greater (by two- to threefold) ability of the mutant to arrest in G_1 relative to the wild-type Ikaros protein (Fig. 5C). Conversely, two previously described Ikaros DNA binding mutants, Ik-2-F3m and Ik-2-F2w (19), exhibited a progressive decrease in their ability to arrest in G_1 that correlated with their DNA binding properties. Ik-2-F2w, with no detectable DNA binding activity (19), was unable to arrest any cells in G_1, whereas the Ik-2-F3m mutant, with reduced affinity for DNA (19), exhibited some activity with respect to the cell cycle control (Fig. 5D).

Taken together, these studies demonstrate that Ikaros's activity to negatively regulate the G_1-S transition can be alleviated by phosphorylation at the p1 region.

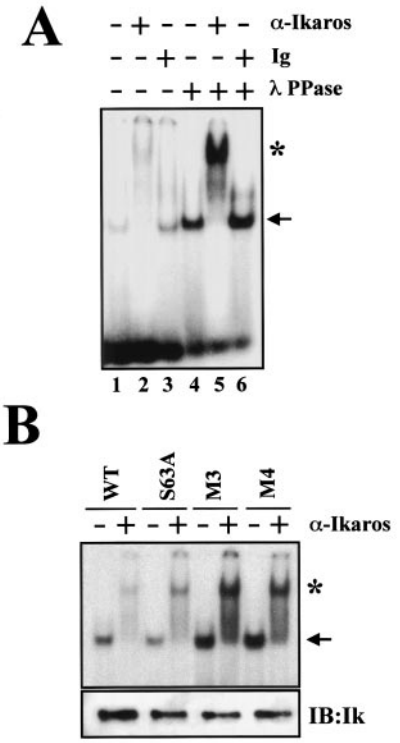

FIG. 6. Ikaros phosphorylation affects DNA binding activity. (A) 293T epithelial cells were transfected with CMV2-FlagIk-1, and nuclear extracts were prepared. After immunoprecipitation, half of Ikaros was dephosphorylated with λ PPase in the immunoprecipitation beads. After removal of the λ PPase by extensive washing, Ikaros was eluted from the beads and assayed for DNA binding. Supershifts were performed by using anti-Ikaros antibody (α-Ikaros) or Ig. (B) Gel shift analysis of indicated Ikaros mutants prepared from 293T cells. The expression levels of Ikaros proteins were analyzed by immunoblotting (IB:Ik). The arrow indicates the specific Ikaros-DNA complex. The asterisk indicates an Ikaros-DNA supershifted complex.

Phosphorylation of Ikaros reduces its DNA binding activity. The DNA binding capacity of Ikaros is required for its biological function (2, 35, 36). Deletion of the Ikaros DNA binding domain facilitates entry into the cell cycle and causes the rapid development of leukemia or lymphoma (2, 36). We therefore examined whether phosphorylation of Ikaros protein, which downmodulates its ability to control the G_1-S transition, influences its DNA binding properties. FlagIk-1 expressed in 293T cells was purified and tested for its DNA binding properties before and after treatment with λ phosphatase (Fig. 6A, lanes 1 and 4). The presence of Ikaros in sequence-specific protein-DNA complexes observed in gel shift assays was confirmed by using Ikaros antibodies or control immunoglobulin (Fig. 6A, lanes 2, 3, 5, and 6). Significantly, dephosphorylation of Ikaros protein increased its affinity for DNA (Fig. 6A, compare lanes 4 to 6 to 1 to 3). Heat inactivation of λ PPase activity abrogated the increase in Ikaros DNA binding activity, confirming that dephosphorylation of Ikaros was the cause of the increase in DNA binding (data not shown).

The effect of Ikaros phosphorylation on DNA binding at positions S63 and the S/T-rich region at positions 385 to 394 was next examined. Wild-type FlagIk-1 and the mutants

FlagIk-1 S63A, FlagIk-1-M3, and FlagIk-1-M4 were expressed and purified from 293T cells. A mutation at position S63 that abrogates one of the major phosphorylation events did not alter the DNA-binding activity of Ikaros (Fig. 6B). However, mutation of the five residues in the S/T-rich region in Ikaros consistently increased its DNA binding by threefold (Fig. 6B, M3). Finally, the combination of S63A and the M3 mutations did not exhibit any compound effect on Ikaros DNA binding (Fig. 6B, M4). Importantly, the two- to threefold increase in the Ik-1-M3 ability to bind DNA correlates with the two- to threefold increase in the protein's capacity to negatively regulate the G_1-S transition.

Thus, Ikaros phosphorylation in exon 8 that occurs during the G_1-S transition decreases the protein's affinity for DNA. This change in Ikaros DNA binding activity may facilitate entry into S phase. Ikaros protein that is unable to be modified at the p1 sites may maintain a higher affinity for DNA and may increase the distribution of cells in the G_1 phase.

DISCUSSION

We have previously shown that reduction in the level of Ikaros and its family members in lymphocytes facilitates lymphocyte activation and causes the rapid development of leukemias and lymphomas, thus classifying these factors as potent tumor suppressors (2, 10, 36). In the present investigation, we provide evidence of new G_1-S-dependent Ikaros phosphorylation events, which downmodulate its ability to control entry into the S phase, possibly by altering its affinity for DNA. Importantly, CKII activity that has been implicated in lymphomagenesis plays a major role in these Ikaros phosphorylation events.

In search of modifications that alter Ikaros activity during the cell cycle, we have identified two major areas of phosphorylation in the Ikaros proteins (p1 and p2). The first (p2) contains a single serine phosphorylation site located in exon 4 at amino acid 63 and is present in a subset of the Ikaros DNA binding isoforms. The second (p1) contains several phosphorylation sites located between amino acids 383 to 404 in exon 8 and is shared by all Ikaros isoforms. These Ikaros phosphorylation events can take place in both lymphoid and nonlymphoid cells, indicating that the kinases involved are not cell type specific, although Ikaros protein expression is tissue restricted. The level of phosphorylation at these sites does appear to vary among different cell types (data not shown), indicating that the signaling pathways involved may be more active in some cells. For example, levels of Ikaros phosphorylation are low in NIH 3T3 cells, which may explain why ectopic expression of Ikaros in these cells exerts a block in the G_1-S transition.

Ikaros phosphorylation undergoes dynamic changes during the cell cycle observed in both cell lines and primary lymphocytes. In the late G_1 phase, the protein is not phosphorylated. Upon transition into the replicative (S) phase, Ikaros becomes phosphorylated. The Ikaros p1 and p2 phosphopeptides and the molecular regulation they may provide are maintained from the replicative through the mitotic phases. Their phosphorylation is lost in the G_1 phase of the next cycle and becomes reestablished during the S phase.

We have previously shown that a reduction in Ikaros levels or deletion of its DNA binding domain in T cells causes their hyperproliferation in response to TCR engagement and accelerates the G_1-S transition (2). Ectopic expression of Ikaros DNA binding isoforms in NIH 3T3 fibroblasts as presented in this study provides further insight into Ikaros's role in cell cycle regulation. Here we have shown that Ikaros blocks the G_1-S transition and that the extent of the block is dependent on Ikaros protein levels. We have also demonstrated that a combination of mutations in the shared Ikaros p1 region that prevents its hyperphosphorylation increases the protein's ability to block the cell cycle in late G_1. Thus, hyperphosphorylation of the Ikaros p1 region is a critical regulatory event that downmodulates the protein's negative effect on the G_1-S transition.

Mutations of S/T residues to negatively charged amino acids are frequently used to provide a phosphomimetic effect (32). Such mutations in the Ikaros major phosphorylation area (residues 383 to 404) failed to reveal such an effect (data not shown). There have been other reports describing S or T substitutions for negatively charged amino acids that were unable to mimic a constitutive phosphorylation state (8, 11, 15, 23). Interestingly, in both Ikaros and these reported proteins, phosphorylation of several residues was involved, and the introduction of negative charges could not substitute for the actual phosphorylation events (8).

Given the previously established hypothesis that Ikaros DNA binding is crucial for its role in development and proliferation, we examined whether the Ikaros p1 and p2 phosphorylation events affected Ikaros's ability to bind DNA in vitro. Mutations in S63 (p2) had no effect on either DNA binding or the stability of the protein. However, mutations in the S/T residues in the region 383 to 404 (p1) increased the ability of the protein to bind DNA by threefold but had no effect on its stability. Since the S/T phosphorylation area lies outside the DNA binding domain, its effect on inhibiting DNA binding must be indirect. Phosphorylation of the Ikaros protein in the p1 region may induce a conformational change that affects the accessibility of the DNA binding domain. Alternatively, p1 phosphorylation may promote interactions with other factors, including components of the previously described Ikaros-associated chromatin remodeling complexes, whose presence may reduce Ikaros's DNA binding.

In search of the kinases responsible for Ikaros phosphorylation, we identified the serine/threonine kinase CKII as a major player. Previous studies have implicated CKII in the regulation of the G_1-S transition (22, 28). Although CKII is constitutively active, its expression is upregulated upon mitogenic stimulation (33). Transgenic mice that express CKII in the thymus and Ikaros-deficient mice both develop T-cell thymomas (29, 36), supporting the hypothesis that functional interactions between these two factors are responsible for T-cell homeostasis. Under this model, CKII phosphorylates Ikaros in the p1 region during the G_1-S transition and reduces Ikaros activity as a negative regulator of this transition. Other kinases, such as cdk2 and GSK3, may also play a role in regulating Ikaros phosphorylation upon entry into the replicative phase of the cell cycle.

Taking into consideration past and current studies, we propose the following models for regulation of Ikaros activity and cell cycle control (Fig. 7). Ikaros impedes the G_1-S transition

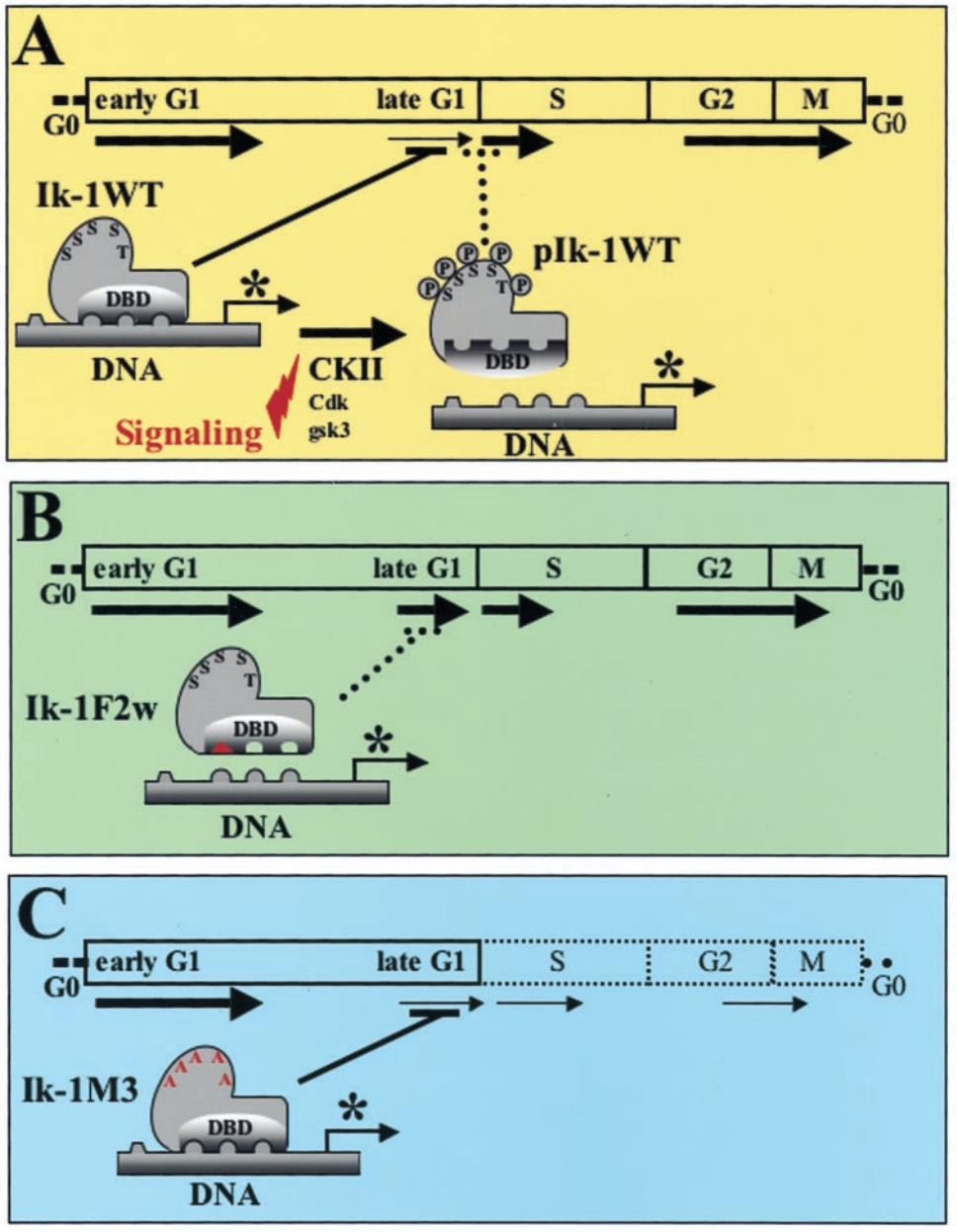

FIG. 7. Models for Ikaros regulation of the G_1-S transition. (A) Ikaros is present in a dephosphorylated state during the late G_1 phase. In this state, Ikaros is active in DNA binding and restricts the G_1-S transition, possibly by regulating transcription of cell cycle regulators (*, in either a positive or negative manner). Phosphorylation by CKII and maybe other kinases in the S/T-rich region in exon 8 reduces Ikaros binding to DNA to facilitate progression through the S phase of the cell cycle. (B) Mutations in the Ikaros DNA binding domain prevent Ikaros from exerting control over the G_1-S transition (by disabling association with the regulatory regions of cell cycle regulators) and cause hyperproliferation and the rapid development of leukemia. (C) Mutations of the phosphate acceptors in exon 8 increase Ikaros DNA binding activity and its ability to impede the G_1-S transition.

by modulating expression of genes that function as positive or negative effectors of the cell cycle (i.e., have a negative effect on cyclins and/or a positive effect on cell cycle inhibitors p27, p21, etc.). Ikaros may affect expression of some of these genes directly by binding to their transcriptional regulatory regions (Fig. 7A). In support of this model, mutations in the Ikaros DNA binding domain alleviate its ability to control the cell cycle (Fig. 7B). Under physiological conditions, Ikaros DNA binding activity is temporarily downmodulated through CKII-dependent phosphorylation of its C-terminal region that facilitates the G_1-S transition (Fig. 7A). Mutations in Ikaros that abolish p1 phosphorylation eliminate this type of regulation on Ikaros DNA binding and block cells in G_1 (Fig. 7C).

The Ikaros exon 8 phosphorylation events described here

first occur during the G_1-S transition but are maintained through the M phase. In a recent study, Dovat et al. (7) have shown that during M phase, Ikaros becomes phosphorylated in the linker region of the DNA binding zinc fingers. These M-phase phosphorylation events also reduce DNA binding of the Ikaros protein and may exclude this family of proteins from binding to mitotic chromosomes (7). Thus, there appears to be a gradual decrease in Ikaros activity during the cell cycle that is affected by phosphorylation. During the G_1-S transition, Ikaros becomes phosphorylated in exon 8, an event that reduces its activity as a negative regulator of the G_1-S transition and its DNA binding. In the M phase, Ikaros becomes phosphorylated at the zinc finger linker regions, which further reduces its DNA binding to possibly exclude it from mitotic chromosomes.

The G_1-S transition is a critical checkpoint in cell cycle regulation. The expression and activity of proteins involved in this transition are tightly regulated, and a failure to do so frequently results in cellular apoptosis or neoplastic transformation (5, 30). In fact, many human cancers present genetic lesions in key regulators of the G_1-phase progression and G_1-S transition (30). Lymphocytes are terminally differentiated cells with the unique property of undergoing proliferative expansions upon encountering antigen. In addition to ubiquitously expressed cell cycle regulators, tissue-specific negative regulators such as Ikaros provide for controlled proliferation of lymphocytes and prevent the development of leukemias. Ikaros modifications may allow only lymphocytes that have received appropriate levels of signaling to enter the replicative phase of the cell cycle. It is tempting to propose that Ikaros's phosphorylation at multiple residues within the p1 region may be responsible for translating different levels of receptor signaling into different levels of Ikaros activity and lymphocyte activation.

The interplay between positive and negative signals that underlies the Ikaros cell cycle-regulated phosphorylation events remains to be elucidated. It will be important to determine whether phosphatases function in concert with CKII and other kinases to provide for the changes in Ikaros phosphorylation detected during the cell cycle. Deregulation of such signaling events in primary lymphocytes may affect the phosphorylation state of Ikaros and its ability to control the cell cycle and thus be responsible for transition to a neoplastic state.

Finally, there are interesting parallels between Ikaros and previously described cell cycle regulators. One of the best-studied tumor suppressors is the nuclear factor Rb, which is involved in the regulation of the G_1-S transition. Rb is inactivated during G_1 by concerted phosphorylation events initiated by different cyclin-cdk complexes, which induce a progressive conformational change in this negative regulator (12). Ikaros also negatively regulates the G_1-S transition, and phosphorylation relieves its ability to do so. However, Ikaros phosphorylation appears to occur later than that of Rb during the G_1-S transition. In addition, Rb phosphorylation affects its interactions with other proteins, whereas Ikaros phosphorylation reduces its ability to bind DNA. It is possible, however, that Ikaros phosphorylation may also affect its interactions with other proteins.

ACKNOWLEDGMENTS

We thank T. Kitamura for the pMX-GFP-IRES vector. We are grateful to A. Liu for technical assistance with gel shifts; Joanne Yetz-Aldape for cell sorting; Taj Pathan for mouse care; and J. Aramburu, B. Morgan, J. M. Redondo, J. Koipally, and the members of the Georgopoulos laboratory for careful reading and valuable comments on the manuscript.

P.G.-D.A. is a Fellow of the Leukemia and Lymphoma Society and was also supported by Ministry of Education and Culture of Spain. K.M. was supported by the Yamanouchi Foundation for Research on Metabolic Disorders and by the Mochida Memorial Foundation for Medical and Pharmaceutical Research. This research was supported by NIH grant RO1-AI380342 to K.G.

REFERENCES

1. **Allman, D., A. Sambandam, S. Kim, J. P. Miller, A. Pagan, D. Well, A. Meraz, and A. Bhandoola.** 2003. Thymopoiesis independent of common lymphoid progenitors. Nat. Immunol. **4:**168–174.
2. **Avitahl, N., S. Winandy, C. Friedrich, B. Jones, Y. Ge, and K. Georgopoulos.** 1999. Ikaros sets thresholds for T cell activation and regulates chromosome propagation. Immunity **10:**333–343.
3. **Boyle, W. J., P. van der Geer, and T. Hunter.** 1991. Phosphopeptide mapping and phosphoamino acid analysis by two-dimensional separation on thin-layer cellulose plates. Methods Enzymol. **201:**110–149.
4. **Channavajhala, P., and D. C. Seldin.** 2002. Functional interaction of protein kinase CK2 and c-Myc in lymphomagenesis. Oncogene **21:**5280–5288.
5. **Classon, M., and E. Harlow.** 2002. The retinoblastoma tumour suppressor in development and cancer. Nat. Rev. Cancer **2:**910–917.
6. **Cortes, M., E. Wong, J. Koipally, and K. Georgopoulos.** 1999. Control of lymphocyte development by the Ikaros gene family. Curr. Opin. Immunol. **11:**167–171.
7. **Dovat, S., T. Ronni, D. Russell, R. Ferrini, B. S. Cobb, and S. T. Smale.** 2002. A common mechanism for mitotic inactivation of C2H2 zinc finger DNA-binding domains. Genes Dev. **16:**2985–2990.
8. **Dulhanty, A. M., and J. R. Riordan.** 1994. Phosphorylation by cAMP-dependent protein kinase causes a conformational change in the R domain of the cystic fibrosis transmembrane conductance regulator. Biochemistry **33:** 4072–4079.
9. **Georgopoulos, K.** 2002. Haematopoietic cell-fate decisions, chromatin regulation and Ikaros. Nat. Rev. Immunol. **2:**162–174.
10. **Georgopoulos, K., M. Bigby, J.-H. Wang, Á. Molnár, P. Wu, S. Winandy, and A. Sharpe.** 1994. The Ikaros gene is required for the development of all lymphoid lineages. Cell **79:**143–156.
11. **Germann, U. A., T. C. Chambers, S. V. Ambudkar, T. Licht, C. O. Cardarelli, I. Pastan, and M. M. Gottesman.** 1996. Characterization of phosphorylation-defective mutants of human P-glycoprotein expressed in mammalian cells. J. Biol. Chem. **271:**1708–1716.
12. **Harbour, J. W., R. X. Luo, A. Dei Santi, A. A. Postigo, and D. C. Dean.** 1999. Cdk phosphorylation triggers sequential intramolecular interactions that progressively block Rb functions as cells move through G1. Cell **98:**859–869.
13. **Harker, N., T. Naito, M. Cortes, A. Hostert, S. Hirschberg, M. Tolaini, K. Roderick, K. Georgopoulos, and D. Kioussis.** 2002. The CD8alpha gene locus is regulated by the Ikaros family of proteins. Mol. Cell **10:**1403–1415.
14. **Ho, A., and S. F. Dowdy.** 2002. Regulation of G_1 cell-cycle progression by oncogenes and tumor suppressor genes. Curr. Opin. Genet. Dev. **12:**47–52.
15. **Huang, W., and R. L. Erikson.** 1994. Constitutive activation of Mek1 by mutation of serine phosphorylation sites. Proc. Natl. Acad. Sci. USA **91:** 8960–8963.
16. **Kim, J., S. Sif, B. Jones, A. Jackson, J. Koipally, E. Heller, S. Winandy, A. Viel, A. Sawyer, T. Ikeda, R. Kingston, and K. Georgopoulos.** 1999. Ikaros DNA-binding proteins direct formation of chromatin remodeling complexes in lymphocytes. Immunity **10:**345–355.
17. **Kitamura, T., and Y. Morikawa.** 2000. Isolation of T-cell antigens by retrovirus-mediated expression cloning. Methods Mol. Biol. **134:**143–152.
18. **Koipally, J., and K. Georgopoulos.** 2000. Ikaros interactions with CtBP reveal a repression mechanism that is independent of histone deacetylase activity. J. Biol. Chem. **275:**19594–19602.
19. **Koipally, J., E. J. Heller, J. R. Seavitt, and K. Georgopoulos.** 2002. Unconventional potentiation of gene expression by Ikaros. J. Biol. Chem. **15:**13007–13015.
20. **Koipally, J., A. Renold, J. Kim, and K. Georgopoulos.** 1999. Repression by Ikaros and Aiolos is mediated through histone deacetylase complexes. EMBO J. **18:**3090–3100.
21. **Krek, W., and J. A. DeCaprio.** 1995. Cell synchronization. Methods Enzymol. **254:**114–124.
22. **Litchfield, D. W.** 2003. Protein kinase CK2: structure, regulation and role in cellular decisions of life and death. Biochem. J. **369:**1–15.
23. **McDowell, J. H., P. R. Robinson, R. L. Miller, M. T. Brannock, A. Arendt, W. C. Smith, and P. A. Hargrave.** 2001. Activation of arrestin: requirement of phosphorylation as the negative charge on residues in synthetic peptides

from the carboxyl-terminal region of rhodopsin. Investig. Ophthalmol. Vis. Sci. **42:**1439–1443.

24. **Molnar, A., and K. Georgopoulos.** 1994. The Ikaros gene encodes a family of functionally diverse zinc finger DNA-binding proteins. Mol. Cell. Biol. **14:** 8292–8303.
25. **Nichogiannopoulou, N., M. Trevisan, S. Naben, C. Friedrich, and K. Georgopoulos.** 1999. Defects in the activity of hemopoietic stem cells in Ikaros mutant mice. J. Exp. Med. **190:**1201–1214.
26. **Nosaka, T., T. Kawashima, K. Misawa, K. Ikuta, A. L. Mui, and T. Kitamura.** 1999. STAT5 as a molecular regulator of proliferation, differentiation and apoptosis in hematopoietic cells. EMBO J. **18:**4754–4765.
27. **Peverali, F. A., T. Ramqvist, R. Saffrich, R. Pepperkok, M. V. Barone, and L. Philipson.** 1994. Regulation of G1 progression by E2A and Id helix-loop-helix proteins. EMBO J. **13:**4291–4301.
28. **Pinna, L. A., and F. Meggio.** 1997. Protein kinase CK2 ("casein kinase-2") and its implication in cell division and proliferation. Prog. Cell Cycle Res. **3:**77–97.
29. **Seldin, D. C., and P. Leder.** 1995. Casein kinase II alpha transgene-induced murine lymphoma: relation to theileriosis in cattle. Science **267:**894–907.
30. **Sherr, C. J.** 2000. The Pezcoller lecture: cancer cell cycles revisited. Cancer Res. **60:**3689–3695.
31. **Sun, L., A. Liu, and K. Georgopoulos.** 1996. Zinc finger-mediated protein interactions modulate Ikaros activity, a molecular control of lymphocyte development. EMBO J. **15:**5358–5369.
32. **Thorsness, P. E., and D. E. Koshland, Jr.** 1987. Inactivation of isocitrate dehydrogenase by phosphorylation is mediated by the negative charge of the phosphate. J. Biol. Chem. **262:**10422–10425.
33. **Vilk, G., D. R. Derksen, and D. W. Litchfield.** 2001. Inducible expression of the regulatory protein kinase CK2beta subunit: incorporation into complexes with catalytic CK2 subunits and re-examination of the effects of CK2beta on cell proliferation. J. Cell. Biochem. **84:**84–99.
34. **Wang, J., A. Nichogiannopoulou, L. Wu, L. Sun, A. Sharpe, M. Bigby, and K. Georgopoulos.** 1996. Selective defects in the development of the fetal and adult lymphoid system in mice with an Ikaros null mutation. Immunity **5:**537–549.
35. **Winandy, S., L. Wu, J. H. Wang, and K. Georgopoulos.** 1999. Pre-T cell receptor (TCR) and TCR-controlled checkpoints in T cell differentiation are set by Ikaros. J. Exp. Med. **190:**1039–1048.
36. **Winandy, S., P. Wu, and K. Georgopoulos.** 1995. A dominant mutation in the Ikaros gene leads to rapid development of leukemia and lymphoma. Cell **83:**289–299.
37. **Zandomeni, R., and R. Weinmann.** 1984. Inhibitory effect of 5,6-dichloro-1-beta-D-ribofuranosylbenzimidazole on a protein kinase. J. Biol. Chem. **259:** 14804–14811.
38. **Zhang, H. S., M. Gavin, A. Dahiya, A. A. Postigo, D. Ma, R. X. Luo, J. W. Harbour, and D. C. Dean.** 2000. Exit from G1 and S phase of the cell cycle is regulated by repressor complexes containing HDAC-Rb-hSWI/SNF and Rb-hSWI/SNF. Cell **101:**79–89.
39. **Zhang, Z.-K., K. P. Davies, J. Allen, L. Zhu, R. G. Pestell, D. Zagzag, and G. V. Kalpana.** 2002. Cell cycle arrest and repression of cyclin D1 transcription by INI1/hSNF5. Mol. Cell. Biol. **22:**5975–5988.